Blasting High-Energy Photons into a Geiger–Müller (G-M) Tube.

Samuel English[1, *]

[1] *Department of Physics, University of California, Santa Cruz, CA 95064, USA*

(Dated: November 27, 2020)

There exist many emergent, macroscopic quantum phenomena associated with the emission of radioactive particles. In particular, with the help of ^{137}Cs source material, we reinforce the logistics of G-M tube circuity as well as the statistical methods and devices which encompass and describe these events accurately. In probing the plateau region of our G-M tube device, we find the plateau voltage $V_P = 840$ V, and the counter threshold $C_T = 560$ mV. In observing the system with some added, parallel external capacitance, we calculate the intrinsic system capacitance $C = 1.294 \times 10^{-9}$ F, net internal resistance $R = 4.033 \times 10^5\,\Omega$, and charge $Q = 1.849 \times 10^{-9}$ C. We investigate Poisson distribution counting statistics and find an expected count rate for radiation emission from our ^{137}Cs source to be 12.74 ± 3.57 counts per second, with $\tilde{\chi}^2_R = 0.375$. We explore the characteristics of our G-M tube's dead time, using both direct and indirect methods. For the former, $\tau = 8 \times 10^{-4} \pm 5 \times 10^{-5}$ s, while for the latter $\tau = 2.47 \times 10^{-2}$ s. Finally, we experiment with lead shielding on the attenuation of gamma rays and conclude that the absorption coefficient $\mu_{obs} = 1.047 \pm 0.02$ cm^{-1} while $\mu_{exp} = 1.6 \pm 0.84$ cm^{-1} (uncorrelated BG case $\tilde{\chi}^2_R = 0.022$).

I. INTRODUCTION

Th theory of how high-energy photons interact with matter predicts the way in which gamma-rays of certain energies are attenuated by lead, as a function of its thickness. In this paper, we strive to measure the rate at which these gamma-rays are attenuated and determine whether the form of this dependence is exponential as expected with previously established concepts in high energy physics.

In total, we wish to cover some basic high-energy particle interactions which are non-trivial, familiarize ourselves with the analysis techniques and instrumentation used in the experimental realm, as well as further refine our statistical skill-set and explore the case of a Poisson process,

Furthermore, our laboratory experiment is quite convenient to study, given the radio-isotope used, cesium-137 (^{137}Cs), which has a half-life of approximately thirty years [1]. This ensures that the radioactivity of these sources does not change measurable throughout the course of our experiment.

In order to actually detect a gamma-ray, the photon must be converted into a high-energy electron or a positron/electron pair (depending on the energy level) to become noticeable. For each energy regime: photoelectric absorption allows conversion to take place at lower energies; Compton scattering dominates the intermediate energies; e+/e- pair production in the field of the nucleus permits conversion at very high energies [1]. Again, charged particles are typically detected by the ionization they produce when travelling through matter. In this experiment, we choose one of the simplest yet reliable detectors, the Geiger–Müller (G-M) tube.

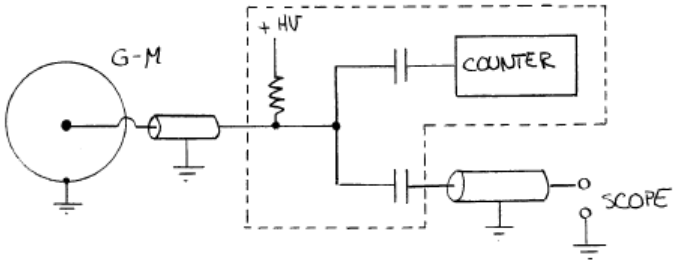

Figure 1. A schematic circuit for observing and counting pulses. The resistor is termed the charging resistor, and the two capacitors block high voltage from entering the counting electronics and oscilloscope, but allow transient pulses through. This setup applies to all experiments conducted [1].

A. Radiation Hazards

We broadly define radiation as any flux of subatomic particles, including photons of all energies, every kind of charged particle (such as beta particles, protons, alpha particles, ions) and uncharged particle such as neutrons.

This radiation, particularly that associated with higher energy, can easily damage biological tissue and material through the process of ionization: the breaking of chemical bonds. The resulting damage is cumulative and linear with respect to the received dose to first order approximation [1]. At lower doses most types of damage can be repaired by the body's natural mechanisms; however, damage to genetic material which reproduces is permanent. This can later manifest itself in the form of cancers, or risk thereof.

Surprisingly, a CT (compute tomography) scan may involve enough ionizing radiation to yield a 1 in 2000 chance of a fatal cancer later in a patient's life. But, looking at the chances provided by cosmic rays and natural radioactive isotopes in the ground, we see that this is on top of a baseline 1 in 5 chance from all other (mostly

* sdenglis@ucsc.edu

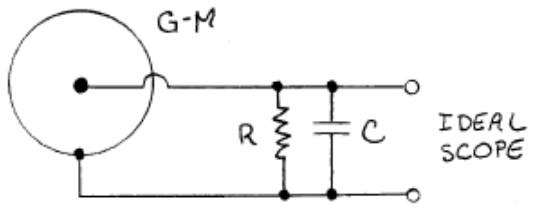

Figure 2. A reduced, equivalent circuit for our G-M tube setup. R is the effective resistance, yielded from the parallel combination of all input resistances and the charging resistance. C is the effective parallel capacitance, given by the parallel combination of the G-M tube's capacitance, the capacitances of all coaxial cables, and the input capacitances of the counter and oscilloscope (Fig. 1), all of which are connected in parallel between ground and the thin anode wire. This reduction in complexity allows for more detailed analysis of circuity and dynamics [1].

natural) causes [1].

We can relay information regarding radiation by two different numbers: the first relates the number of particles emitted by the source, called its *activity*, and is usually measured in *Curies*, where a single Curie is defined to be 3.7×10^{10} disintegrations per second; the next type is more complicated, relating the effects produced by the radiation in a number called *roentgen*, the amount of gamma radiation producing a specific amount of ionization per cm^3 of medium through which it travels, and *rem* (roentgen equivalent mammal), which illustrates the amount of radiation which, when absorbed by mammalian tissue, would produce the same biological effects as the absorption of 1 roentgen of gamma or X-ray radiation [1].

In this laboratory assignment, our ^{137}Cs sources are on the order of 10 micro-Curies, which is relatively harmless. Even if swallowed, the outcome would be around 2 millirem (mr) — about the same dosage as provided by cosmic rays in 140 hours spent at sea level, or in making a single transcontinental flight [1].

B. Geiger–Müller (G-M) Tube

1. Circuitry Logistics

Our SPECTECH counter provides a high voltage to the G-M tube and reads the output pulses, which are temporary drops in the charge on the innermost wire due to the current associated with each pulse event. We subsequently split the signal and pass it on to an oscilloscope which displays the shape of the pulses. Fig. 1 illustrates our setup [1]. The dashed line encapsulates all components within the SPECTECH counter box. The diagram also depicts the coaxial cable running from G-M tube to counter box, and from counter box to oscilloscope. These cables include a grounded shield, which ends up contributing to the overall capacitance of the system.

There exists some *plateau voltage* at which the count rate no longer significantly increases upon increasing voltage thereafter; and, the corresponding pulse height is called the *threshold amplitude* (Fig. 3).

When some charge Q builds up on the anode, it fuels an effective capacitance C, which is a combination of the capacitance stemming between the wire (anode) and shell (cathode), the capacitances of the coaxial cables as previously described, as well as the input capacitances of the counter and oscilloscope, all connected in parallel between ground and the thin anode wire [1].

The charge Q previously built up then discharges through the parallel resistances (from the charging resistor and input resistances of the counter and oscilloscope, which combine to form a net resistance R). In a simplified model, we can leave out the voltage supply as shown in Fig. 2 since the voltage across the blocking capacitors remains close to constant during this entire process.

For our experimental purposes, we assume a realistic scenario in which the discharge resistance is finite. In this case, the change in voltage from both electrons and ions returns to zero with an exponential time constant τ equal to RC. Therefore, if we connect a capacitor C_K with some known capacitance in parallel with our output, we obtain the following expressions for the time constant τ and amplitude A:

$$\begin{aligned} \tau &= R\,(C + C_K) \\ A &= \frac{Q}{(C + C_K)} \end{aligned} \tag{1}$$

If we instead connect some known resistor R_K in parallel with the output, we obtain the equation set

$$\begin{aligned} \tau &= C\,\frac{(RR_K)}{(R + R_K)} \\ A &= \frac{Q}{C} \end{aligned} \tag{2}$$

We can see that an external capacitance will increase the time constant and decrease the pulse amplitude by that same factor. In contrast, an applied external resistance will reduce the time constant but will not necessarily affect the amplitude of pulses.

2. Dead Time

After a particles passes through the G-M tube and discharges, readings on the counter will be disabled for a short period of time, typically on the order of several hundreds of microseconds for the tube we will be using [1]. This "dead time" required to re-establish a high voltage and recombine ionized gas within the tube causes particles which pass through during its effect to not register. At this point, counts will become anti-correlated with one another, and the application of Poisson statistics breaks

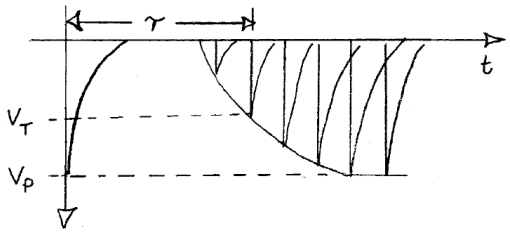

Figure 3. Theoretical image of pulses on oscilloscope reading. V_P represents the pulse amplitude, V_T is the trigger threshold. Illustrates the dead time for a primary G-M tube event [1].

down.

To estimate this quantity, we may either approach things directly or indirectly.

For the former, we may observe pulses from the beta particles of our source at a high enough voltage such that pulse height is roughly twice the counter threshold amplitude [1]. By examining the oscilloscope trace, we may observe and estimate the dead time noting that pulses detected too soon after the primary event will not develop to their full amplitudes (Fig 3). Consequentially, the effective dead time of our counter electronics will depend upon the nominal pulse height as well as the counter threshold for triggering the pulses.

For the latter, we may estimate the dead time using the following line of reasoning: if we reach sufficiently high counting rates the G-M tube will be in a dead time state a significant portion of the time, thus lowering the apparent count rate. Let us consider that some m number of particles per second enter the G-M tube with an associated dead time τ, and that some n pulses per second are registered by the counter box [1]. For any single given second, the tube will be dead for $n\tau$ seconds, and, conversely, will be alive for $1 - n\tau$ seconds. Using our elbow grease to solve all the algebra we obtain equations for both m and n:

$$m = \frac{n}{1 - n\tau} \quad \text{and} \quad n = \frac{m}{1 + m\tau} \tag{3}$$

We duly note the second equation implies that if $m\tau \gg 1$, n will become significantly reduced; while, if $m\tau \ll 1$, the dead time effects become negligible, leading $n \approx m$.

Because of the dead time's characteristics, we know that the count rates of two samples put together will strictly be less than the sum of the individual rates [1]. Suppose that m_a and n_a are the actual counting rates for some sample a, that m_b and n_b are those for some sample b, and that m_{ab} and n_{ab} are those for the two counted together. Since $m_{ab} = m_a + m_b$, we can write

$$\frac{n_{ab}}{1 - n_{ab}\tau} = \frac{n_a}{1 - n_a\tau} + \frac{n_b}{1 - n_b\tau},$$
$$0 = \frac{n_a}{1 - n_a\tau} + \frac{n_b}{1 - n_b\tau} - \frac{n_{ab}}{1 - n_{ab}\tau} \tag{4}$$

Where we then define $a \equiv n_a$, $b \equiv n_b$, and $c \equiv n_{ab}$ so

$$0 = \frac{[a(1 - b\tau) + b(1 - a\tau)](1 - c\tau) - c(1 - a\tau)(1 - b\tau)}{(1 - a\tau)(1 - b\tau)(1 - c\tau)}$$

Using our algebra skills and elbow grease once again, we derive the following equations and conclusions:

$$\begin{aligned} 0 &= a[1 - c\tau - b\tau + bc\tau^2] \\ &+ b[1 - c\tau - a\tau + ac\tau^2] \\ &- c[1 - a\tau - b\tau + ab\tau^2] \end{aligned}$$

$$\begin{aligned} 0 &= a - \cancel{ac\tau} - \underline{ab\tau} + abc\tau^2 \\ &+ b - \cancel{bc\tau} - \underline{ab\tau} + \cancel{abc\tau^2} \\ &- c + \cancel{ac\tau} + \cancel{bc\tau} - \cancel{abc\tau^2} \end{aligned}$$

$$\begin{aligned} 0 &= a + b - c - 2ab\tau + abc\tau^2 \\ \tau &= \frac{2ab \pm \sqrt{4a^2b^2 - 4(abc)(a + b - c)}}{2abc} \\ &= \frac{1 \pm \sqrt{1 - \frac{c}{ab}(a + b - c)}}{c} \end{aligned}$$

Thus, plugging back in values for a, b, and c we find an exact and approximate solution for τ

$$\begin{aligned} \tau &= \frac{1 \pm \sqrt{1 - \frac{n_{ab}}{n_a n_b}(n_a + n_b - n_{ab})}}{n_{ab}} \\ \tau n_{ab} &= 1 - \left[1 - \frac{n_{ab}(n_a + n_b - n_{ab})}{n_a n_b}\right]^{\frac{1}{2}} \end{aligned} \tag{5}$$

$$\tau \approx \frac{n_a + n_b - n_{ab}}{2n_a n_b} \tag{6}$$

C. Poisson Distribution & Counting Statistics

Radioactive nuclei such as our ^{137}Cs source are unstable, meaning they tend to decay and have some finite lifetime. The exact moment at which any particular nucleus will decay is not precisely predictable; it is a chance event due to quantum effects. If we pick some nucleus and observe it for a time interval Δt, there is a probability p that our nucleus would decay within that given time interval, proportion to Δt:

$$p = \beta \Delta t \tag{7}$$

where β is some constant of proportionality. Each decay event is completely independent of all others, regardless of the specimen's age or memory.

Given N number of nuclei present at some $t = 0$, where N is sufficiently large, some of them will decay during a time interval Δt. We chose the mean number of nuclei

which decay to be represented by ΔN. So, we would then expect ΔN to equal pN; in other words:

$$\frac{\Delta N}{N} = -\beta \Delta t \tag{8}$$

where the negative sign indicates that ΔN decrements in N's value. Given a infinitesimally small Δt, we can then integrate Eq. (8) to find the mean number of nuclei $N(t)$ remaining for any given time t:

$$N(t) = N_0 e^{-\beta t} \tag{9}$$

where N_0 is the amount of nuclei present at $t = 0$. When $t = \frac{1}{\beta}$, the nucleus reaches its *mean lifetime*, which happens to be around 43.3 years for ^{137}Cs.

The rate at which an unstable nucleus decreases happens to be the rate at which products of decay are produced [1]. If a ^{137}Cs nucleus decays, we should observe a single gamma ray's production. Thus, we can say that gamma rays are produced at a mean rate

$$-\frac{d}{dt}N(t) = \beta N_0 e^{-\beta t} = \beta N(t) \tag{10}$$

We highlight that if we reduce our count time span to an interval much shorter than the mean lifetime of the nucleus, the function $N(t)$ will remain practically constant, and gamma rays will be produced at an essentially constant mean rate as well.

Due to our imperfect setup and the nature of the geometry of our apparatus, we are only able to fully capture and count a fixed fraction of the total gamma rays produced by our ^{137}Cs source [1]. The detector will only monitor a small fraction of N, we'll call it n, with a mean rate given by

$$\frac{dn}{dt} = \epsilon \beta N \tag{11}$$

where ϵ represents the small fraction of gamma rays actually caught by the detector.

By simple algebraic manipulation, we see that in any given time interval Δt our G-M tube will be able to detect Δn gamma rays:

$$\Delta n = \epsilon \beta N \Delta t \tag{12}$$

We choose to let m be Δn, some integer number of counts recorded. Due to the probabilistic nature of the decay phenomenon, we expect to see fluctuations in m over counting intervals.

To encapsulate these events more precisely, we show that the probability that m particles will be counted in some Δt is given by the *Poisson Distribution* function:

$$P(m) = e^{-\lambda}\frac{\lambda^m}{m!} \tag{13}$$

where the long-term average count rate λ can be estimated by suitably extensive data collection.

The Poisson Distribution function $P(m)$ has the following properties:

1. It is normalized:

$$\sum_{m=0}^{\infty} P(m) = e^{-\lambda}\sum_{m=0}^{\infty}\frac{\lambda^m}{m!} = e^{-\lambda}e^{\lambda} = 1 \tag{14}$$

2. The mean or average value of m is λ:

$$\begin{aligned}\sum_{m=0}^{\infty} mP(m) &= e^{-\lambda}\sum_{m=1}^{\infty} m\frac{\lambda^m}{m!} = e^{-\lambda}\sum_{m=1}^{\infty}\frac{\lambda^m}{(m-1)!} \\ &= \lambda e^{-\lambda}\sum_{m=1}^{\infty}\frac{\lambda^m - 1}{(m-1)!} = \lambda e^{-\lambda}\sum_{k=0}^{\infty}\frac{\lambda^k}{k!} \\ &= \lambda e^{-\lambda}e^{\lambda} = \lambda\end{aligned} \tag{15}$$

which we obtain by re-indexing $k = m - 1$ and then cancelling based on exponential series. λ is called the *population mean*. Assuming an infinite number of time intervals testes, the mean value of m would approach and then equal exactly λ.

3. The population variance is also λ:

$$\sigma^2 = E(X^2) - (E(X))^2 = \sum_{m=0}^{\infty}(m-\lambda)^2 P(m) \tag{16}$$

We reduce the issue to a calculation of $E(X^2)$ since $(E(X))^2$ is already known:

$$\begin{aligned}E(X^2) &= \sum_{m=0}^{\infty} m^2 e^{-\lambda}\frac{\lambda^m}{m!} = \lambda e^{-\lambda}\sum_{m=1}^{\infty} m\frac{\lambda^{m-1}}{(m-1)!} \\ &= \lambda e^{-\lambda}\left(\sum_{m=1}^{\infty}\frac{(m-1)\lambda^{m-1}}{(m-1)!} + \sum_{m=1}^{\infty}\frac{\lambda^{m-1}}{(m-1)!}\right) \\ &= \lambda e^{-\lambda}\left(\lambda\sum_{m=2}^{\infty}\frac{\lambda^{m-2}}{(m-2)!} + \sum_{m=1}^{\infty}\frac{\lambda^{m-1}}{(m-1)!}\right) \\ &= \lambda e^{-\lambda}\left(\lambda\sum_{i=0}^{\infty}\frac{\lambda^i}{i!} + \sum_{j=0}^{\infty}\frac{\lambda^j}{j!}\right) \\ &= \lambda e^{-\lambda}(\lambda e^{\lambda} + e^{\lambda}) \\ &= \lambda(\lambda + 1) \\ &= \lambda^2 + \lambda\end{aligned} \tag{17}$$

Then:

$$\begin{aligned}\sigma^2 = var(X) &= E(X^2) - (E(X))^2 \\ &= \lambda^2 + \lambda - \lambda^2 \\ &= \lambda\end{aligned} \tag{18}$$

Thus, the population variance $\sigma^2 = \lambda$ for the mean value $(m-\lambda)^2$ where an infinite number of intervals considered.

As it turns out, the Poisson distribution function governs any collection of random events which are uncorrelated. We know now that the standard deviation σ is given by $\sqrt{\lambda}$, and that as λ becomes sufficiently large, the Poisson distribution becomes well-approximated by the Gaussian distribution [1], with the same $\sigma = \sqrt{\lambda}$:

$$P_G(m) = \frac{1}{\sigma\sqrt{2\pi}} e^{\frac{-(m-\lambda)^2}{2\sigma^2}} \tag{19}$$

D. Photon Attenuation

When charged particles move continuously along their path of travel, they steadily lose energy by ionizing atoms along the way. Statistically, there is a range that a charged particle with a given energy can travel inside of a given material before it is stopped completely. If we know the energy, we thereby can deduce how much shielding is necessary to block the barrage of charged particles [1].

Individual gamma rays do not gradually lose energy along their path; instead, they go right through a material unscathed until it randomly, strongly interacts with an electron or atom. We expect an individual gamma ray to either (1) scatter from the inline beam, deflect, (2) become totally absorbed, (3) continue on unaffected [1]. While, in principle, scattering can either increase or decrease the detector's count rate, we will assume that both absorption and scattering will equally remove photons from the beam.

So, an incident beam of emitted gamma rays with intensity I on a slab of material of thickness Δx will attenuate its energy by an amount that is proportion to both Δx and I:

$$\Delta I = -\mu I \Delta x \tag{20}$$

where μ, a proportionality constant, is called the *absorption coefficient*. Assuming the entire beam of gamma ray photons have the same energy, μ would be a constant, and Eq. (20) can be integrated to yield the following:

$$I = I_0 e^{-\mu x} \tag{21}$$

Where this function in Eq. (21) yields a beam intensity I after having traversed a total absorbent thickness x, where I_0 represents the incident intensity. μ will always have inverse units of length, since the quantity $\mu\Delta x$ must be dimensionless. It is important to note the probabilistic nature of this phenomenon: there is no memory as to how much shielding material has been passed through or how much time has passed, the probability of an interaction is constant [1].

It is often useful to think of the absorption coefficient *per atom*, as denoted by σ, where we expect μ to be proportional to the number of nuclei or atoms per unit volume of absorbent material:

$$\mu = \frac{N\rho\sigma}{A} \tag{22}$$

where A is the atomic weight of the absorbent ($\frac{mass}{mole}$), N is Avogadro's number ($\frac{atoms}{mole}$), ρ is the absorbent's density ($\frac{mass}{volume}$), leading σ to substantiate an *atomic cross-section* in units $\frac{cm^2}{atom}$.

We then define a quantity $\frac{\mu}{\rho}$ called the *mass absorption coefficient* in units $\frac{cm^2}{gram}$, which is useful when comparing different absorbencies for different materials:

$$\mu x = \frac{\mu}{\rho}\rho x \tag{23}$$

There are three processes mainly responsible for gamma ray absorption and photon attenuation [1]:

1. Pair production—the gamma ray passes near the nucleus and converts into an electron-positron pair, which only occurs when the it has a sufficient amount of energy (1.022 MeV or higher).

2. Photoelectric absorption—the gamma ray is absorbed completely upon ejection of a bound electron from the atom with an energy comparable to that of the photon's.

3. Compton scattering—the gamma ray reflects or bounces off an electron in the atom, ejecting the electron but continuing to travel with reduced energy and altered direction.

Thus, the total absorption coefficient μ can we defined as the sum of all three contributions:

$$\mu = \mu_{pair} + \mu_{photo} + \mu_{compton} \tag{24}$$

Each of these processes have an associated atomic cross-section, and probabilities can be accurately calculated for certain setups. We know that lead is particularly good for shielding due to its atomic number rather than its mass density, as the gamma-ray energy goes further out of resonance with lead's K-shell electron binding energy [1]. Again, strange phenomena may occur due to this, such as if the detector is fairly close, lead shielding will tend to enhance and overestimate the attenuation of the count rate due to Compton cross-sections.

E. Error Propagation & Statistical Methods

In order to propagate error, we utilize the general formula for error propagation, given the term we wish to isolate an uncertainty for $f(x_1, .., x_N)$:

$$\sigma_{x_i} = \sqrt{\sum_{i=1}^{N} \left(\frac{\partial f}{\partial x_i} \sigma_{x,i} \right)^2} \tag{25}$$

Eq. (25) applies to any function of multiple variables. So, we apply this idea to each of our calculated values dur-

ing this laboratory experiment, and find the uncertainty associated with each.

In general, for a weighted average, the weighted value, weight parameter, and deviation of the weighted average are defined as

$$x_w = \frac{\sum_{i=1}^{N} x_i w_i}{\sum_{i=1}^{N} w_i}, \quad w_i = \frac{1}{\sigma_{x,i}^2} \tag{26}$$

$$\sigma_{\bar{x},wav} = \frac{1}{\sqrt{\sum_{i=1}^{N} w_i}} \tag{27}$$

where x_w is the weighted average of some parameter x, w_i is the weighting on the average calculation, and $\sigma_{\bar{x},wav}$ represents the uncertainty on our new, weighted parameter of x.

II. APPARATUS AND PROCEDURE

A. Plateau Region

Using the circuit configuration seen in Fig. 1, we place our ^{137}Cs source near the G-M tube, connect the G-M tube to the output of the SPECTECH counter, and then connect and record channel 1 of the oscilloscope to the SIGNAL output of our counter box. We observe and plot the amplitude of the pulses and the count rate as we increase the tube voltage over a range of roughly 400 to 1000 Volts. When we hit a high voltage where the count rate no longer tends to increase, we call this the *plateau voltage*, and the corresponding pulse height the *threshold amplitude* [1].

B. Intrinsic G-M Tube Capacitance & Resistance

We connect a known capacitance C_K in parallel across the counter input and then measure the amplitude and time constants of each pulse, with and without the capacitor. From these values, we are able to determine the intrinsic total capacitance C, the charge Q, and the intrinsic net resistance R, as seen visually in our idealized circuit configuration in Fig. 2.

Next, we remove the external capacitor and instead substitute a known resistance. We will notice how the pulses become much shorter in amplitude. In principle, we could redo our calculations obtained from the known capacitance; in practice, this will not yield a good answer, since the RC time constant is so small compared to the drift time of the ions to the cathode that our pulse shape is no longer perfectly exponential [1].

C. Background Counting Rate

There exist many other sources other than the sealed source which emit radiation and trigger our G-M tube's counting box. Most mainly come from muons (cosmic rays showering the atmosphere) as well as nearby radioactive sources in building materials or the underneath and inside earth itself [1]. We measure the background counting rate by removing all immediate sources of radiation from the G-M tube.

D. Counting Statistics & Poisson Distribution

We confirm that the probability distribution of counts in several single-second intervals from the G-M tube resembles the theoretical Poisson distribution's form.

So, we place our source such that roughly five to ten counts per second are detected, and then record the counts for 100 one-second intervals.

From this data, we make a plot of the frequency distribution $F(m)$ versus m where $F(m)$ is the fraction of one-second intervals showing a given number of m counts. We will obtain the mean for our sample of measurements $\bar{m}$, which is the best estimate for λ, which we use in our Poisson distribution calculations.

We compare the observed frequency distribution $F(m)$ values with the expected frequency distribution $P(m)$ by using the χ^2 goodness of fit test.

E. G-M Tube Dead Time

To obtain values for the G-M tube dead time, we employ both direct and indirect methods. From our data, we estimate the dead time for pulses with amplitude roughly twice the counter threshold amplitude which we determine in III A or Fig. 4.

Similarly, we use the expressions derived previously in Eq. (5) and Eq. (6) in order to obtain better estimates on our dead time τ. Using both sources, we record counts for both individually and then both together. Again, the high voltage should be set such that pulses have roughly twice the counter threshold amplitude.

We compare both values for the dead time τ, for the direct and indirect methods of obtaining a final result.

F. Gamma Ray Lead Absorption

By setting various amount of lead sheets between the source and detector to absorb gamma rays, we are able to measure the counting rate as a function of the absorber thickness ρx:

$$\rho x = \frac{\rho x a}{a} = \frac{M}{a} \tag{28}$$

where M is the mass of a lead sheet and a is the area of that sheet. This method of calculating the thickness of the material turns out to be much more accurate than using the measured physical thickness [1].

While the distance between source and detector should never change during this experiment, we will be varying the absorber thickness by at least three absorption lengths (three centimeters). Ensuring our source currently isolated gamma rays to exclusively emit, we begin by comparing the count rate with no lead at all to the count rate with 1 mm of lead. As discussed in I D, the rate will tend to increase; thus, we should use a minimum lead shielding of around 3 mm to make this effect become negligible [1].

Moving forwards, we proceed to measure the count rate with several different thicknesses of lead, each data point separated by 5 mm to ensure for seven data points spanning roughly 30 mm.

We ensure a longer period to obtain a count rate as the lead thickness increases, as to obtain a small fractional error $\frac{\sqrt{N}}{N}$ at each target lead thickness.

Let us not forget yet another important point to take into account: the background radiation. The background count rate is NOT negligible in comparison to the counting rate with our largest lead thickness [1].

Subtracting background before plotting, we make a graph of $\ln I$ vs. x to find out if it looks linear as we would expect. Then, using a least-squares linear regression, we fit a model to our data set without subtracting background to a function which is the sum of an exponential that decays with x and a constant representing the background count rate.

We then compare our measured value of μ with the theoretical value provided and extracted from section IV.

III. RESULTS AND DISCUSSION

A. Plateau Region

We employ the procedure enlisted in II A, and are able to carefully extract values for the plateau voltage as well as the counter threshold amplitude. In varying the high voltage over a range of 400 to almost 1000 volts as seen in Fig. 4, we discover that the count rate tends to approach a value of 14 counts with sufficiently high, applied voltage. Furthermore, using this plateau voltage value $V_P \approx 840$ V, we then obtain a counter threshold voltage or amplitude $C_T \approx 560$ mV, the pulse amplitude which is sufficiently large enough to be routinely picked up by our SPECTECH counter.

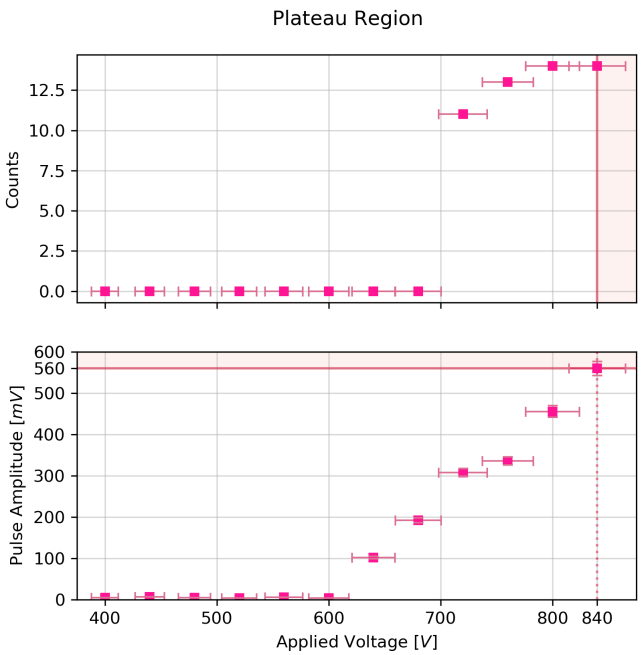

Figure 4. Side-by-side illustration of the G-M tube's plateau region for high voltages. The upper region demonstrates the terminal nature of count rate when met with a sufficiently high voltage, termed the *plateau voltage*, $V_P \approx 840$ V. Below, we see a *threshold amplitude* or counter threshold, $C_T \approx 560$ mV, at which the pulse amplitude is sufficiently large enough to be routinely detected by our counting box.

B. Intrinsic G-M Tube Capacitance & Resistance

Using the structure and procedure seen in II B, we calculate values for the G-M tube's intrinsic capacitance and net resistance. Through the use of equation sets Eq. (1) and Eq. (2), we are able to algebraically solve for R, C, Q_{wc}, and Q_{nc}, where both Q's are calculated independently for the with and without capacitor cases:

$$\begin{aligned} R &= \frac{\tau_{wc} - \tau_{nc}}{C_K} \\ C &= \frac{\tau_{nc}}{R} \\ Q_{wc} &= A_{wc}(C + C_K) \\ Q_{nc} &= A_{nc}C \end{aligned} \tag{29}$$

where τ represents the time constant (ms), C_K is the external capacitance ($1.8nF$), A is the amplitude of pulse (V), subscript$_{wc}$ means *with* external capacitor, and subscript$_{nc}$ means *no* external capacitor.

We conclude that our system's intrinsic capacitance $C = 1.294 \times 10^{-9}$ F, our net internal resistance $R = 4.033 \times 10^{5}\,\Omega$, and our expected charges $Q_1 = 1.758 \times 10^{-9}$ C and $Q_2 = 1.941 \times 10^{-9}$ C. Taking a simple average between the two, under the assumption that both cases should lead to the same answer, we obtain a final charge $Q = 1.849 \times 10^{-9}$ C or 1.85 nC.

Again, we duly note how the pulses become much shorter in amplitude when we remove the external capacitor and instead substitute a known resistance.

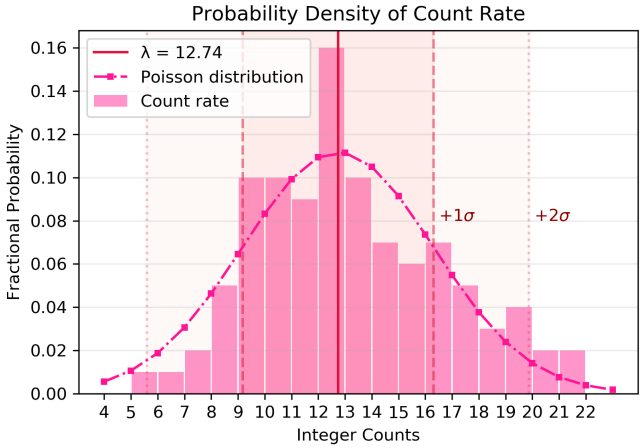

Figure 5. Plot of fractional probability distribution versus integer count rate, visually comparing and contrasting our raw input data and an theoretical Poisson distribution function. We find $\lambda = 12.74$, and that our Poisson approximation model suits our observations very well, with $\tilde{\chi}^2_R = 0.375$.

C. Background Counting Rate

After practicing the proper scientific etiquette of II C and using our due diligence, we find the measured background counting rate to be $R_B = \frac{122}{301}$ counts per second. That is, we expect to witness an unphysical number of 0.405 events per second, or 2.47 seconds pass between each recorded event, on average.

D. Counting Statistics & Poisson Distribution

Utilizing the procedure of II D, we create a probability density of count rates plot as illustrated by Fig. 5. Here, we see the stark resemblance of our raw input data and the theoretical Poisson distribution function.

With great reason to believe our predicted fit ($\tilde{\chi}^2_R = 0.375$), we learn that our average count rate $\lambda = 12.74$. Thanks to the earlier exercises completed in confirming Poisson distribution properties, we can further solidify our understanding of the situation (II C). Given our Poisson model is accurate for our observed data set, we easily extract σ, since $\sigma^2 = \lambda$, leading to the additional information highlighted in Fig. 5.

So, our observed distribution must govern a collection of random events which are each uncorrelated, given that it closely follows a Poisson distribution. We can then say with certainty that our expected count rate for radiation emission from our ^{137}Cs source is 12.74 ± 3.57 counts per second given our mentioned experimental setup.

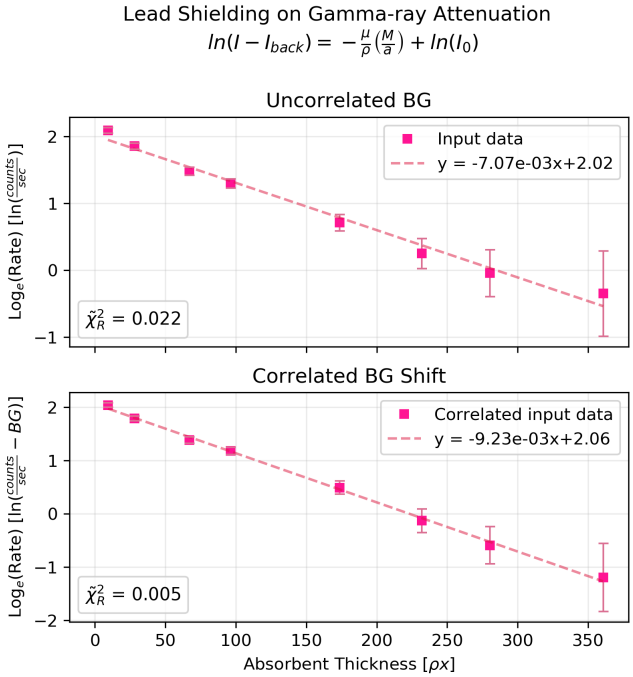

Figure 6. Linear fits for lead shielding on gamma-ray attenuation (log of count rate versus absorbent thickness). Upper region displays a regression for raw input data with no compensation for background (BG) counting rate (uncorrelated), lower region illustrates input data including the BG shift (correlated). Both yield some linear expression which contains a slope and intercept parameter with associated errors. The uncorrelated BG case $\tilde{\chi}^2_R = 0.022$, correlated BG shift $\tilde{\chi}^2_R = 0.005$.

E. G-M Tube Dead Time

Upon observation of the pulses from our source's emitted beta particles at sufficiently high voltage, we directly estimate the dead time $\tau = 8 \times 10^{-4} \pm 5 \times 10^{-5}$ s noting that pulses detected too soon after a primary event will not develop to their full amplitudes.

Following the indirect method explained in detail in I B 2, and the main equations referenced in II E, we obtain better estimates on our dead time τ. With the help of our tricky, indirect method and algebra skills we estimate $\tau = 2.47 \times 10^{-2}$ s.

F. Gamma Ray Lead Absorption

Carefully observing the structure outlined in II F, we craft a graphic illustrating the effect of lead shielding on gamma-ray attenuation as seen in Fig. 6. In order to fit a linear regression to our input data, we must first take the natural logarithm of both sides of our equation:

$$\ln\left(I - I_{back}\right) = -\frac{\mu}{\rho}\left(\frac{M}{a}\right) + \ln\left(I_0\right) \tag{30}$$

where we note that $-\frac{\mu}{\rho}\left(\frac{M}{a}\right)$ reduces to $-\mu x$ for simplicity. This ensures for a simple yet precise model for our observations.

In general, it is important to ensure untainted results and conclusions drawn from our experiments and sets of data: if we accidentally introduce biases or unwarranted correlations into our data, we can no longer trust our results as legitimate. Thus, in analyzing Fig. 6, we tend to trust the upper region far more than the lower. While the correlated background (BG) shift may seem to fit a linear regression much more accurately ($\tilde{\chi}^2_R = 0.005$) than the uncorrelated BG case ($\tilde{\chi}^2_R = 0.022$), we may not trust the former for the aforementioned reasons.

So, in concluding a value for our absorption coefficient μ, we choose to compare Fig. 6's upper plot to the theoretical value extracted from section IV. With proper slope conversion and consideration of ρ, we find that $\mu_{obs} = 1.047 \pm 0.02$ cm^{-1} while $\mu_{exp} = 1.6 \pm 0.84$ cm^{-1}. This fits well within our tolerance range, meaning we have further reason to trust our findings.

IV. CONCLUSIONS

At the end of the day, we have been able to reinforce the logistics of G-M tube circuitry and their innerworkings, as well as the emergent, macroscopic quantum phenomena associated with the emission of radioactive particles from a source material.

In Fig. 4 we illustrate the plateau region of our G-M tube device and record the plateau voltage $V_P = 840$ V, and the counter threshold $C_T = 560$ mV.

Then, in III B, we discover that the intrinsic system capacitance $C = 1.294 \times 10^{-9}$ F, our net internal resistance $R = 4.033 \times 10^5\,\Omega$, and our final charge result $Q = 1.849 \times 10^{-9}$ C or 1.85 nC. We, again, note how the amplitude decreases shortly after substituting an external resistance rather than capacitance.

Later, we record the background counting rate $R_B = \frac{122}{301}$ counts per second. That is, we expect to witness an unphysical number of 0.405 events per second, or 2.47 seconds pass between each recorded event, on average.

We next investigate Poisson distribution counting statistics and perform a chi-square goodness of fit test on our data as fully demonstrated by Fig. 5. In plotting our fractional probability distribution versus the integer count rate, we discover that our expected count rate for radiation emission from our ^{137}Cs source is 12.74 ± 3.57 counts per second, with a modest accuracy statistic $\tilde{\chi}^2_R = 0.375$.

We explore the quantities and characteristics of our G-M tube's dead time, using both direct and indirect methods. For the former, we recover $\tau = 8 \times 10^{-4} \pm 5 \times 10^{-5}$ s, while with the latter we estimate $\tau = 2.47 \times 10^{-2}$ s. We are keen to notice that the direct method of observation seems to muddle results, ultimately underestimating the magnitude of dead time τ.

Finally, we experiment with lead shielding on the attenuation of gamma rays in our series of trials with varying absorber thicknesses. Taking advantage of Eq. (30) and glancing at Fig. 6, we solidify our findings and conclude that $\mu_{obs} = 1.047 \pm 0.02$ cm^{-1} while $\mu_{exp} = 1.6 \pm 0.84$ cm^{-1}. This fits well within our tolerance range, meaning we have further reason to trust our findings; furthermore, the linear fit used to extract a slope parameter for μ had a precise chi-square test statistic for the uncorrelated BG case $\tilde{\chi}^2_R = 0.022$.

We hope to have solidified the reader's understanding of these phenomena, and to have conveyed our analysis and conclusions in an accurate as well as thoughtful manner. Further data taking or cross-checked calculations could be carried out to reinforce the legitimacy of our findings.

ACKNOWLEDGMENTS

SE is a part of the PHYS 133, Intermediate Laboratory course. None of this information is presented for journal publication, only for writing improvement.

BIBLIOGRAPHY

[1] George Brown. *Laboratory Manual: Physics 133*. University of California, Santa Cruz, Spring 2020.

APPENDIX

Photon energy MeV	Photo-electric σ_{PE}	Compton σ_C	Pair formation σ_{PF}	Total σ_T	Coefficient per cm, μ, cm^{-1}	Mass coefficient μ/ρ $\mathrm{cm}^2/\mathrm{gm}$
0.1022	1782	40.18		1822	59.9	5.30
0.1277	985	38.01		1023	33.6	2.97
0.1703	465	35.04		500	16.4	1.45
0.2554	161	30.70		192	6.31	0.558
0.3405	75.7	27.63		103.3	3.39	0.300
0.4086	47.8	25.74		73.5	2.42	0.214
0.5108	27.7	23.50		51.2	1.68	0.149
0.6811	14.5	20.73		35.2	1.16	0.102
1.022	6.31	17.14		23.45	0.771	0.0682
1.362	3.86	14.81	0.1948	18.87	0.620	0.0549
1.533		13.91	0.3313			
2.043	2.08	11.86	1.247	15.19	0.499	0.0442
2.633						
3.065		9.313	3.507			
4.086	0.369	7.761	5.651	14.28	0.469	0.0415
5.108	0.675	6.698	7.560	14.93	0.491	0.0434
6.130		5.917	9.119			
10.22	0.316	4.115	14.04	18.47	0.607	0.0537
15.32	0.206	3.042	18.00	21.25	0.698	0.0618
25.54	0.122	2.044	23.24	25.41	0.835	0.0739

Figure 7. Absorption cross sections and coefficients for lead [1].